NUMERICAL SIMULATION OF A LOW POWER ARCJET THRUSTER*

Andrea Santovincenzo‡, William D. Deininger¥ and Gaetano De Lorenzo§
FiatAvio - Comprensorio BPD
00034, Colleferro (Rm), ITALY

Vito Salvatore¶ and Annamaria Russo Sorge#
DISIS - Dipartimento di Scienza ed Ingegneria dello Spazio
Università degli Studi "Federico II"
Napoli, Italy

ABSTRACT

This paper provides a description of a numerical model for low power arcjet internal flow field simulation. The modeling needs and approach are illustrated, followed by a discussion of the main hypotheses at the basis of the model. Then a full description of the equations is given and the model boundary conditions are presented. Representative results of the simulated flow field in the constrictor and nozzle of a low power, hydrogen arcjet are then given. At a hydrogen mass flow rate of 7.5 mg/s the code has predicted a specific impulse of about 900s at an efficiency of 35% for operation at 1 kW. The validity and limitations of the results are outlined and planned future improvements are summarized.

NOMENCLATURE

ASPT-3	Advanced Space Technology Program 3
B	Third body
c_i	Concentration of species i
c_p	Specific heat at constant pressure, J/K
DISIS	"Dipartimento di Scienza ed Ingegneria dello Spazio" (Space Science and Engineering Department)
D_{im}	Multicomponent diffusion coefficient of species i, m^2/s
D_{ij}	Binary diffusion coefficient, m^2/s
ESA	European Space Agency
$\underline{E}$	Electric field, V/m
E_d	Dissociation energy , J
E_i	Ionization energy , J
E	Emissive flux, W/m^2
e	Electron
k_B	Boltzmann constant, J/K
K	Equilibrium constant
h	Panck's constant, Js, enthalpy, J/kg
I	Total current, A
$\underline{j}$	Electric current density, A/m^2
m	Particle mass, kg
$\dot{m}$	Mass flow rate, kg/s
M	Molecular weight
n	Number density, m^{-3}
$\dot{n}$	Net production rate, $m^{-3}s^{-1}$
N	Avogadro's number, 1/mole
p	Pressure, Pa
P	Electrical power, W
R	Universal gas constant, J/mole/K
R	Radiosity, W/m^2
s	Scattering coefficient per unit length
S_{rad}	Radiative loss, W/m^3
T	Temperature, K
Th	Thrust, N
u,v,w	Cylindrical components of velocity, m/s
$\underline{V}$	Velocity vector
x	Mole fraction
z,r,θ	Cylindrical coordinates

Greek letters

α	Absorption coefficient per unit length
ϕ	Electric potential, V
η	Efficiency
κ	Thermal conductivity, W/m^2K
μ	Coefficient of viscosity, Ns/m^2
ρ	Mass density, kg/m^3
σ	Electrical conductivity, mho/m
τ	Viscous stress tensor
$<\sigma v>$	Janev's reaction rate coefficient
Φ	Viscous dissipation function, W/m^3
$\overline{\Omega}_{ij}^{(l,m)}$	Average effective collision integral, m^2

Subscripts

an	anode

---

* Presented as Paper Number IEPC-97-011 at the 25th International Electric Propulsion Conference, August 24-28, 1997, Cleveland, Ohio, USA
‡ Engineer, Member AIAA
¥ Senior Scientist, Manager, Electric Propulsion Department, Associate Fellow AIAA
§ Engineer, Electric Propulsion Department
¶ Engineer
# Associate Professor, Aerospace Propulsion

cat	cathode
ch	chemical
e	electrons
em	electro-magnetic
h	heavy species
rad	radiative
t	total

INTRODUCTION

FiatAvio-BPD undertook development and ground testing of low power arcjet thrusters within the framework of the ESA ASTP-3 program starting in the 1990. Much experimental work was devoted to characterization and performance optimization of the engines[2,3]. It was noted that expensive empirical work could be reduced by means of a numerical tool able to provide performance prediction and a deeper understanding of the complex local thermofluid-dynamic phenomena of the arcjet flow.

Starting from these needs, FiatAvio-BPD in collaboration with DISIS at the University of Naples "Federico II" began an internally funded activity devoted to the build-up and tuning of an arcjet internal flow numerical code. A multidimensional code was desired which was able to simulate multispecies non-equilibrium flow for many different propellants and to provide details on electromagnetic field in the constrictor region. The inclusion of turbulence effects and radiative inner exchange completes the model.

As an output, design strategies for thruster cooling are also given.

In order to reduce the implementation effort, the code has been structured as a set of independent routines attached to a commercially available core fluid dynamic open solver, the CHAM Ltd. distributed PHOENICS code. The routines can be separately activated to obtain solutions with increasing physics complexity[4].

STATE OF ART

Despite of their ease of use and capabilities to provide reasonable arcjet performances estimates, quasi-one-dimensional models[15,16] present serious limitations concerning the details of the gas physics and flow dynamics. Therefore, they can not provide many useful indications to an arcjet designer from an industrial point of view.

Multidimensional models [6,7,8,18,19,20] are more relevant to practical arcjet design needs.

The older two-dimensional models assumed that electron and gas temperatures were equal. Butler and King[18] developed a 2-D model that can deal with various propellants and includes chemical kinetics. The Rhodes and Keefer model [19] covers the whole arcjet and incorporates full transport effect calculations. It also includes radiation escape and radiation diffusion, but the overall significance of radiation appears to be small, especially in a low power arcjet. In Italy, the group working at the University of Pisa[17] has reported arcjet modeling work using hydrazine as the propellant.

Two-temperature models[6,7,8,20] have recently been used in simulations by Miller and Martinez Sanchez[6], Burton and Krier [7], Babu et al.[8], Fujita and Arakawa[20], etc, to account for thermal non-equilibrium, caused by the large difference in masses between particles. They found that significant energy losses have been neglected using simplifying assumptions about thermal and chemical equilibrium. Their models allow electrons to have a separate temperature. The presence of molecular species in appreciable quantities may give rise to a non-Maxwellian or non-Boltzmann electron energy distribution in the plasma[8,22]. This may suggest that multi-energy models[22], rather than multi-temperature models, would be appropriate in some cases. While this is expected to be the case for heavy propellants, such as N_2 and N_2H_4, hydrogen may be described adequately by one temperature[8]. As in other models, these authors include flow-swirl, although its role appears to be minor.

Arc attachment at the anode is a troublesome. A better understanding of the physics of the discharge in the region around the attachment to the electrode surfaces is a key to understanding such issues as arc behavior and electrode erosion. The progress from artificial ionization or a conductivity floor[18] through electron diffusion[6,8,20] as a mechanism for conduction to the anode wall, appears to have resolved several issues for argon while leaving several unresolved issues for H_2 and N_2.

Simple models for the voltage drops at anode and cathode have been included recently by Fujita and Arakawa[20] and Miller and Martinez-Sanchez[6].

Arc instabilities are another unresolved issue in numerical simulation of arcjet flow fields. While anode and cathode attachments are quite stable, instabilities can occur under certain conditions and around the boundaries of the envelop of stable operation[22]. These instabilities may be very destructive if realized during engine operation. The relationship between arc phenomena, gas flow pattern, electrode surface physics is not clearly understood.

Despite of all progress, the confidence in arcjet models in not yet sufficient to allow their use for design. At present, inadequacy in the understanding of non-equilibrium processes, arc instabilities and arc/electrode attachment regions is thought to be of greatest importance[22].

MODEL

The assumptions and model are summarized below.

Basic assumptions

Navier-Stokes equations govern viscous supersonic flow. These equations become considerably more complicated for arcjets which include an electric arc since they must include heat generation, species diffusion, chemical reactions and variable transport properties.

In view of the basic phenomenology of thrust generation in an arcjet, the system of equations behavior must be strongly driven by energy equation; it must model the energy transfer from electric arc to gas, the energy redistribution within internal modes of the propellant molecules, the conversion to global kinetic energy of the gas and the radiative and convective heat losses to wall.

To take into account these effects, the effort was addressed towards developing a good formulation of the source terms in the energy equation; they include an ohmic dissipation term depending on the current density field and in turn on the voltage distribution, a term incorporating non-equilibrium dissociation and ionization of propellant, and an inner radiative exchange term.

Computation of sources lies on solving a set of auxiliary differential equations including a simplified electromagnetic Maxwell equation, species diffusion equations, and a radiative flux equation.

In theory any kind of propellant can be simulated by the model. Nevertheless, the more complex the molecular structure of the gas the harder it is to represent the non-equilibrium chemical phenomena. As a starting point, an hydrogen arcjet has been selected to be modeled because of its relatively simple chemistry and kinetics and the ready availability of data in literature.

Both dissociation and ionization phenomena have been taken into account and a four species mixture gas, including H_2, H, H^+, e^- has been assumed to flow through the thruster. Dissociation has been assumed to be caused by collisions of molecular hydrogen with heavy species and with electrons and ionization process has been described by inelastic collision and third-body recombination[7,8].

In accordance with the work of Babu[8] on hydrogen arcjets, thermal non-equilibrium has not been accounted for and so one single temperature energy equation was considered for both the heavy species (neutrals and ions) and for electrons.

Moreover, further simplification was obtained introducing the hypothesis of dynamic coupling between neutrals and ions that provides for a single heavy species velocity.

Radiative losses prediction, although not fundamental to arcjet main physical features description, could be very effective from a design point of view.

Then it was decided to include the composite radiosity model[9] in the arcjet flow simulation in which a function, the composite radiosity, representing the average of the incoming and outgoing radiation fluxes over all directions of the solid angle, is computed by solving an additional ordinary differential equation. The source term in the energy equation is directly derived from the radiosity model.

Standard κ-ε turbulence equations can be also attached to the main system of equations to better simulate viscous effects in the constrictor and in the nozzle region. Nevertheless, only small improvements in the quality of solution have been noted in spite of a significant increase in the computational time. This is probably due to the need of a recalibration, in this case, of the constants used in the κ-ε equations. The coupling of electromagnetic forces and flow turbulence, that may influence arc stability, requires the inclusion of an additional term describing electromagnetic effects in the turbulence modeling[22]. This coupling has not been considered in this initial model.

Analytical Model description

Following the above assumptions, a set of equations has been solved. They include:

Fluid Dynamic Equations

- Global Continuity

$$\nabla \cdot (\rho \underline{V}) = 0$$

- Momentum

$$\nabla \cdot (\rho \underline{V}\underline{V}) + \nabla \cdot \underline{\underline{\tau}} = 0$$

- Species Conservation Equations

Mass conservation of species is derived by two diffusion equations: one for atomic hydrogen and one

for electrons, by the plasma neutrality condition and by the global continuity.

For electron and hydrogen, respectively

$$\nabla\cdot(\rho\underline{V}c_e)-\nabla\cdot(\rho D_e\nabla c_e)=S_e$$

$$\nabla\cdot(\rho\underline{V}c_H)-\nabla\cdot(\rho D_H\nabla c_H)=S_H$$

in which the source terms are given, for ionization, by the generalized model of ionization and three body recombination[7]:

$$S_e = m_e\dot{n}_e$$

$$\dot{n}_e = Rn_e\left(Sn_H - n_e^2\right)$$

with R and S functions of temperature:

$$S=\left(\frac{2\pi m_e k_B T_e}{h^2}\right)^{\frac{3}{2}}\exp\left(-\frac{E_i}{k_B T_e}\right)$$

$$R = 6.985\cdot10^{-42}\exp\left[\frac{\left(\ln\frac{T}{1000}-4.0833\right)^2}{0.8179}\right]$$

and, for dissociation, by

$$S_H = m_H\left(\dot{n}_H + \langle\sigma\upsilon\rangle n_e n_{H_2} - \dot{n}_e\right)$$

where the production term for atomic hydrogen can be expressed as:

$$\dot{n}_H = ANT^{\eta}\exp\left(-\frac{E_d}{\hat{R}T}\right)\left(a_H[H]+a_{H_2}[H_2]\right)\left\{[H_2]-\frac{1}{K_N}[H]^2\right\}$$

where:

$AT^{\eta}\exp\left(-\frac{E_d}{\hat{R}T}\right)=k_f$, forward rate constant[10],

K_N : equilibrium constant based on concentration[10],

a_H, a_{H2}: third body ratios, representing the third body efficiency in the involved reaction[11]

and $\langle\sigma v\rangle$ is the Janev's reaction rate coefficient[8,12] (function of T).

The dominant chemical reactions in hydrogen plasma for this model are given in the Table A, in which B is any third body involved in the reaction.

Ionic hydrogen population is derived from plasma quasi-neutrality equation,

$$n_e = n_{H^+}$$

while molecular hydrogen, H_2, population is derived from overall continuity, or equivalently from

$$\sum_i c_i = 1$$

- Energy Equation

$$\nabla\cdot(\rho\underline{V}h_t)-\nabla\cdot\kappa\nabla T = -\nabla\cdot\underline{V}\cdot\underline{\underline{\tau}}+S_{em}+S_{ch}+S_{rad}$$

In it the source terms are expressed as follows:

$$S_{em}=\left|\underline{j}\right|^2/\sigma$$

taking into account ohmic dissipation, and

$$S_{ch}=-\tfrac{1}{2}E_d\dot{n}_H - E_d\langle\sigma v\rangle n_e n_{H_2} - E_i\dot{n}_e$$

taking into account for species fractions.

Chemical reactions in the model
For molecular hydrogen
$H_2+e\rightarrow H+H+e$
$H_2+B\rightarrow H+H+B$
$H_2+e\rightarrow H^+ +H+e+e$
For atomic hydrogen
$H+e\rightarrow H^+ +e+e$
$H+B\rightarrow H^+ +B+e$
$H+H+B\rightarrow H_2+B$

Table A: Chemical reaction in the model

Radiative equations

$$S_{rad}=\alpha\cdot[R-E]$$

in which the composite radiosity function $\mathcal{R}$ fulfills the following equation:

$$\nabla\cdot\left[\frac{4}{3(\alpha+s)}\nabla R\right]+\alpha\cdot(E-R)=0$$

Electromagnetic equations

Electromagnetic equations are derived by the general Maxwell set of equations assuming that neither external nor self-induced magnetic fields are present and that the electron pressure gradient be negligible. This results in an irrotational electric field, that coupled with simplified Ohm's law, brings to a Poisson like equation for the electric potential [6].

Ohm's law and current conservation are used to solve for j and electric potential ϕ:

$$\nabla\cdot(\sigma\nabla\phi)=0$$

$$\underline{E} = -\nabla\phi$$

$$\underline{j} = \sigma \underline{E}$$

Transport Properties.

In the global system of equations, transport coefficients are strongly dependent from temperature and pressure of mixture and from pure species mass fractions.

In the computation presented here averaged values for transport coefficients, extracted from experimental data set, were used.

In species conservation equations, a multi-component diffusion coefficient must be used[10] for the diffusion species i through the mixture. The multi-component diffusion coefficient is related to the binary diffusion coefficient D_{ij} for the species i into j by means of an approximate expression:

$$D_{im} = \frac{1 - x_i}{\sum_{j \neq i} \frac{x_j}{D_{ij}}}.$$

The values of viscosity and thermal conductivity must be found from the values of μ_i e κ_i of each of the chemical species i through some mixture rules.

For viscosity[10], (Wilke's rule),

$$\mu = \sum_i \frac{n_i \mu_i}{\sum_j n_j M_{ij}},$$

where

$$M_{ij} = \sqrt{\frac{2m_{ij}}{m_i}} \frac{\overline{\Omega}_{ij}^{(2,2)}}{\overline{\Omega}_{ii}^{(2,2)}},$$

$$m_{ij} = \frac{m_i m_j}{m_i + m_j} \text{ reduced mass,}$$

while for pure species[13] i,

$$\mu_i = 2.6693 \cdot 10^{-26} \frac{\sqrt{M_i T}}{\overline{\Omega}_{ii}^{(2,2)}}.$$

For thermal conductivity of the mixture, Wilke's rule can be used again, replacing μ with κ and μ_i with κ_i, where κ_i can be expressed[13] as

$$\kappa_i = 1.9891 \cdot 10^{-25} \frac{\sqrt{\frac{T}{M_i}}}{\overline{\Omega}_{ii}^{(2,2)}}$$

In the above expressions $\overline{\Omega}_{ij}^{(l,m)}$ stands for the average effective collision integral. The values required in the calculation of transport coefficients are interpolated from data reported in Ref.13 and Ref.14.

The electrical conductivity values are taken as an interpolated function of temperature from experimental data both by Ref.13 and by Ref.15.

NUMERICAL METHOD

Integration method

Due to the nature of the core solver, an upwind Finite Volume discretization approach has been used for the system of equations creating an algebraic set but strongly non-linear system to be solved iteratively.

The code encompasses a fully-implicit method named SIMPLEST (Semi-Implicit Method for Pressure-Linked Equations ShorTened) which acts guessing the pressure field, solving for the other variables and using the resulting residuals of the continuity equation as quantitative indicators of corrections which should be made to the pressure and velocity fields. To avoid much under-relaxation, required to drive convergence and to improve pressure field prediction, the influence coefficients in the pressure corrections contain only diffusion contributions, whereas the convection terms are added in the continuity errors of the cells. The discretization of the convection terms is obtained by an upwind-differencing scheme which is first order accurate in space but is robust and it overcomes instability problem and unrealistic oscillations during the solution. The terms representing diffusion are discretized assuming that the property gradient and transport properties which they multiply are uniform over cell faces. The gradients are based on the supposition that the properties vary linearly and the transport properties are arithmetic or harmonic averages of those or either side of the cell faces.

Additional information about SIMPLEST method can be found in Ref.9.

Boundary conditions

Appropriate boundary conditions must be specified on the boundary of the domain, along with suitable initial conditions.

At the inlet boundary, the gas is assumed to enter the domain axially and with no velocity component in the azimuthal direction. The mass flow rate, the temperature and the pressure are specified, while gas density is derived from the ideal gas law

and the axial velocity component is calculated from the continuity equation.

The outflow boundary is represented by the exit cross section of the nozzle, therefore the flow is assumed to be supersonic.

The boundary conditions for the voltage are shown in Table B. The anode and the cathode are modeled as equipotential surfaces, with the voltage calculated to obtain the specified current I. The axial gradient of the voltage is set to zero at the inflow and outflow boundaries so the current is enforced to attach within the arcjet thruster.

The boundary conditions for the energy equation are also shown in Table B. The anode temperature is held constant at 1000 K, while the cathode temperature is held at 1100K along is straight side and increases to 3600 along its sloping face of the tip. These wall temperatures are kept constant during the computations.

Symmetry conditions are imposed along the thruster centerline.

variable	inlet	outlet	cathode	anode
v	0	extrapolated	no slip	no slip
w	from continuity	extrapolated	no slip	no slip
T	specified	extrapolated	specified	specified
P	specified	extrapolated	$\partial P/\partial \bar{n} = 0$	$\partial P/\partial \bar{n} = 0$
ϕ	$\partial\phi/\partial z = 0$	$\partial\phi/\partial z = 0$	$\phi=\phi_{cat}$	$\phi=\phi_{an}$

Table B: Boundary Conditions

ARCJET GEOMETRY AND GRID

To allow for future comparisons with experimentally available data, the geometry of a low power hydrazine arcjet, denoted MOD-B, has been assumed since it has been extensively tested at FiatAvio-BPD in the past. A schematic diagram of the arcjet is reported in Fig. 1. This thruster has a constrictor diameter and length of 6 mm, a nozzle half-angle of 19 deg. and an exit diameter of 60 mm.

The arcjet chamber and nozzle has been discretized by a 40 X 95 cells structured body fitted coordinates axysimmetric mesh, built through a grid generator that makes use of attraction functions as well as stretching of the grid line distribution.

The grid used is reported in Fig. 2.

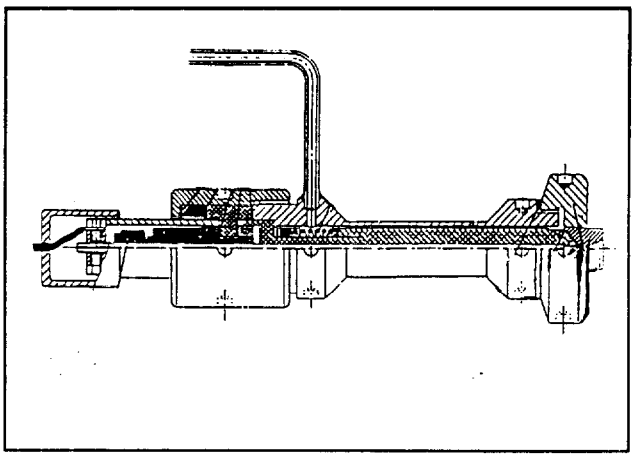

Fig. 1: Low Power Arcjet at FiatAvio-BPD

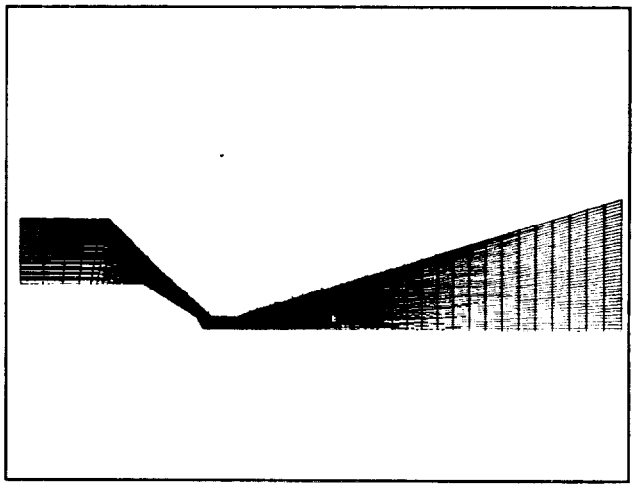

Fig. 2: Computational grid

RESULTS

Up to now only axisymmetric runs were performed neglecting the representation of swirling injection of propellant at inlet; yet, due to the features of the core solver used in the simulation, a relatively quick extension to 3-D case is allowed.

Simulation run times are about 20 hours on a IBM RISC 6000 computer.

Plot of current density is presented in Fig. 3. A sharp maximum can be seen in the cathode tip region near the arc, following the arc path. The current density, and hence, the ohmic heating, are larger in the constrictor. These effects can be seen in Fig 4, where the temperature contour plot is shown. In fact, the temperature remains fairly constant in the convergent region then increases significantly inside the constrictor region because of the high energy input into the flow due to the ohmic dissipation. The maximum temperature of 12,400 K occurs near the cathode tip. As the flow enters the divergent nozzle,

the temperature quickly drops as a consequence of the expansion process. It should be noted that the lines are almost parallel to the thruster axis, revealing the strong radial gradients inside the constrictor, so that two separated flow regions can be individuated.

Velocity profiles, shown in Fig. 5, indicate the high flow speeds reached in the hot flow region, near the centerline of the thruster. A very thick boundary layer is also present in accordance with theoretical predictions. In the nozzle the flow path is affected by strong expansion downstream the geometrical discontinuity between constrictor and nozzle.

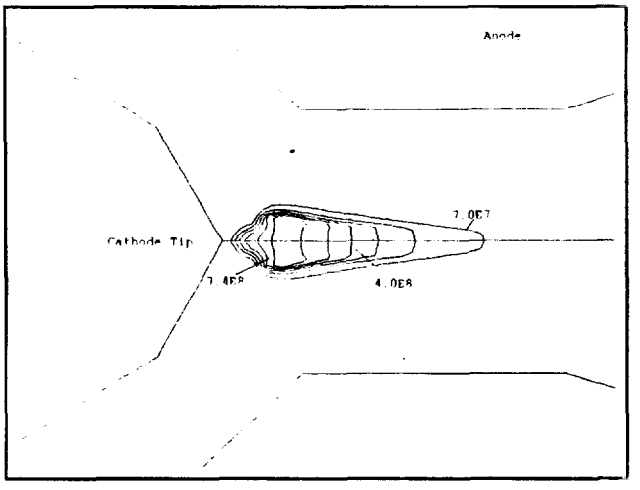

Fig. 3 Contours of Current Density

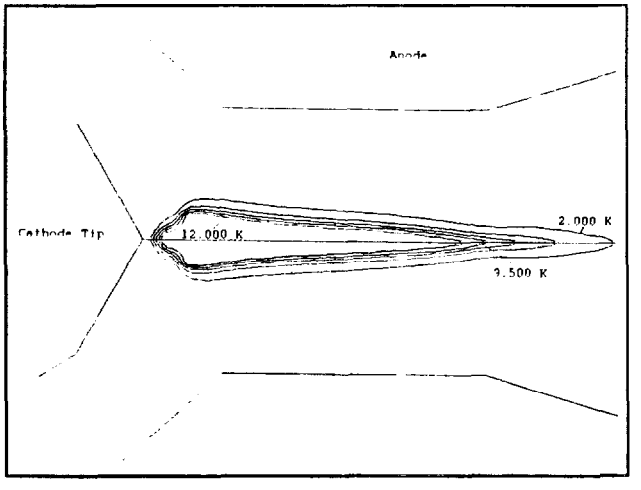

Fig. 4 Contours of Temperature

The computed performance for $\dot{m} = 7.5$ mg/s is given in Table C.

Efficiency is estimated [21], by: $\eta = \frac{Th^2}{2\dot{m}P}$.

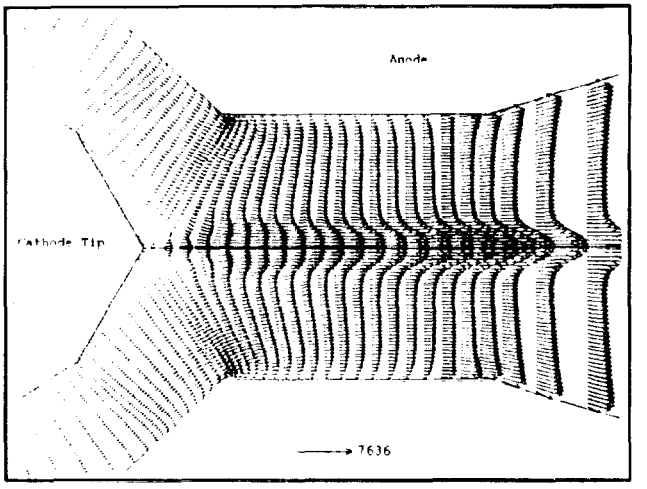

Fig. 5 Velocity Profiles

Thruster Performance	
Mass Flow Rate	7.5 mg/s
Arc Current	10 A
Power	1 kW
Specific Impulse	900 s
Efficiency	35 %

Table C: Thruster Performance

CONCLUSIONS

A numerical model for the analysis of the internal flow field of a low power arcjet thruster, developed by FiatAvio-BPD in collaboration with University of Naples, has been presented. The multidimensional, turbulent, radiative Navier-Stokes equations are employed. The modeling of electromagnetic effects has been limited to ohmic heating contribution effects in the energy balance equation. A detailed description of the arc structure and attachment mechanism has not been included.

The presented results are relative to a first simplified model in which averaged values of transport coefficients, extracted from experimental data set, and a reduced chemical source term for energy equation were used.

A qualitative and a basic quantitative agreement between the model calculations and the literature data indicates that the model accounts for the essential physics of the flow and heat addition processes. Nevertheless, the main limitations of the simulation are the underestimation of transport coefficients and

then of diffusion effects, the lack of details in arc path representation and a oversimplification of chemical effects that can alter the values of temperature in the constrictor region.

These results represent a first step toward the implementation of a more complete model, incorporating a more accurate description of electromagnetic effects, that includes electron pressure gradient driving terms in the electromagnetic equation, and a better description of transport coefficients and non-equilibrium chemistry.

ACKNOWLEDGEMENTS

This work is based on the degree thesis of Vito Salvatore, at University of Naples "Federico II"

The activities at BPD were supported through an internally funded research and development program.

The authors would like to thank P. Bellomi of FiatAvio-BPD for helpful discussions during the implementation of the model.

REFERENCES

1. Deininger, W. D., Attili, M. "Electric Propulsion and Plasma Applications at BPD" , 46th International Astronautical Congress, IAF-95.S.3.08, 1995
2. Cruciani G. and Deininger W. D., 'Development Testing of a 1 kW Class Arcjet Thruster', AIAA-92-3114, 28th JPC, July 1992
3. Di Stefano R., Deininger W. D., Tosti E., 'Performance Testing of a 1 kW Arcjet Using Hydrazine', IEPC-93-082, 23rd International Electric Propulsion Conference, Seattle,. 1993
4. Baiocco, P and Bellomi, P., "A Coupled Thermo-Ablative and Fluid Dynamic Analysis for Numerical Application to Solid Propellant Rockets", 31st AIAA Thermophysics Conference, New Orleans, LA, 1996
5. Martinez-Sanchez M. and Miller S. A.. 'Arcjet Modeling: Status and Prospects', Journal of Propulsion and Power, Vol 12, No.6, Nov-Dec 1996.
6. Miller, S. A. and Martinez-Sanchez, M., 'Nonequilibrium Numerical Simulation of Radiation-Cooled Arcjet Thruster', IEPC-93-218, 23rd International Electric Propulsion Conference, Sept. 1993
7. Burton, L.R. Krier, H., Megli, T.W., Bufton, S.A. and Tiliakos, N.T.., "Fundamentals of Arcjet Thruster Thermophysics", Technical Report UILU-ENG 95-0508, Sep. 95
8. Babu V., Aithal S. M., Subramaniam V. V., 'Numerical Simulation of a Hydrogen Arcjet', Journal of Propulsion and Power, Vol 12, No 6, Nov-Dec 1996.
9. Spalding D. B., 'Mathematical Modeling of Fluid-Mechanics, Heat Transfer and Chemical Reaction Processes: a Lecture Course', CFDU, Imperial College of Science and Technology, Jan 1980
10. Anderson J.D., 'Hypersonic and High temperature gas dynamics', McGraw-Hill, 1989
11. Rogers, R. C., Schexnayder C. J., 'Chemical Kinetic analysis of hydrogen-air ignition and reaction times', NASA-TP 1856, 1981
12. Janev R. K., Langer W.D., Evans, K. And Post, D.E. 'Elementary Processes in Hydrogen-Helium Plasmas', Springer Verlag, New York, 1987
13. Grier, N.T. , "Calculation of transport Properties of Ionizing atomic Hydrogen", NASA TN D-3186, April 1966
14. Vanderslice, J.T., Weissman, S., Mason, E.A. and Fallon, R.J. , "High-Temperature Transport Properties of Dissociating Hydrogen", Physics of Fluids, Vol.5, No.2, Feb. 1962, p. 155-164
15. Glocker, B., Schrade, H.O., and Sleziona, P.C., "Numerical Prediction of Arcjet Performance", AIAA 90-2612, AIAA/DGLR/JSASS, July 1990
16. Glocker, B., Schrade, H.O., and Auweter-Kurtz, M., "Performance Calculation of Arcjet Thruster – The Three Channel Model," IEPC 93-187, 23rd International Electric Propulsion Conference, Seattle, 1993
17. Andrenucci, M., Scortecci, F. ,Capecchi, G. and Wunsch, T. , "Decelopment of a Computer Programme for the Analysis of Arcjet Nozzle," IEPC 91-113, 21st International Electric Propulsion Conference, Viareggio, 1991
18. Butler, G.W., Kull, A.E., and King, D.Q., "Single and Two Fluid Simulation od a Low Power Hydrogen Arcjets," AIAA Paper 94-2870, June 1994.
19. Rhodes, R. and Keefer, D., "Non-equilibrium Modelling of Hydrogen Arcjet Thruster," IEPC 93-217, 23rd International Electric Propulsion Conference, Seattle, 1993.
20. Fujita, K., and Arakawa, Y., "Numerical Prediction of Arcjet Performance Based on the Chemical Kinetics and Electron Temperature Disparity," IEPC 95-025, 24th International Electric Propulsion Conference, Moscow, 1994.
21. Butler, G.W. and Cassidy, R.J., "Directions for Arcjet Technology Development," Journal of Propulsion and Power, Vol 12, No 6, Nov-Dec 1996.
22. Birkan, M.A., " Arcjets and Arc Heaters: An Overview of Research Status and Needs", Journal of Propulsion and Power, Vol 12, No.6, Nov-Dec 1996.